3D PHYSICAL VERSUS EMPIRICAL MODELS FOR HR SENSOR ORIENTATION AND ELEVATION EXTRACTION: EXAMPLES WITH IKONOS AND QUICKBIRD

Th. Toutin [a,]*, P. Schauer[b]

[a] Natural Resources Canada, Canada Centre for Remote Sensing, 588 Booth St., Ottawa, Ontario, K1A 0Y7 Canada - thierry.toutin@ccrs.nrcan.gc.ca

[b] Technische Universität Dresden, Institut für Kartographie, Helmholtzstraße 10, D-01062, Dresden, Germany - Regen_Schauer@gmx.de

Commission I, WG I/5

KEY WORDS: Photogrammetry, Ikonos, QuickBird, Stereoscopic, DEM/DTM, Accuracy

ABSTRACT:

Elevations for digital surface model (DSM) generation were extracted from different stereo high-resolution (HR) images (QuickBird and Ikonos) using 3D physical and empirical geometric models. The 3D physical model is *Toutin's* model (TM) developed at the Canada Centre for Remote Sensing, and the empirical model is the rational function model (RFM). First, Vendor-supplied RFMs refined with polynomial functions and TM were compared for the sensor orientations with least-squares adjustments with different number of ground control points (GCPs). TM and RFMs gave similar results with Ikonos as soon as RFM was refined with a shift computed from at least one GCP. On the other hand, TM gave better results than RFMs with QuickBird regardless of the number of GCPs. Due to relief dependency, QuickBird RFM needed to be refined at least with linear functions computed from at least 6-10 GCPs. Some large errors were, however, noted on forward image RFM in column. The stereo-extracted elevations of DSMs were then compared to 0.2-m accurate Lidar elevation data. Because DSM stereo-extracted elevations included the height of land covers (trees, houses), elevation linear errors with 68 percent confidence level (LE68) were computed for the entire area and three land-cover classes (forested, urban/residential, bare surface). TM and RFMs with Ikonos, regardless of the method and GCP number, achieved comparable results for all classes while TM achieved overall better results than RFMs with QuickBird. All results demonstrated the necessity of refining Ikonos RFM with a tri-directional shift and at least one GCP but QuickBird RFM with 1st order linear functions and 6-10 GCPs.

RÉSUMÉ :

Des altitudes pour la création de modèles numériques de surface (MNS) ont été restituées à partir de deux couples stéréoscopiques de haute résolution (QuickBird et Ikonos) en comparant deux modèles géométriques 3D : un physique et un empiriques. Le modèle physique 3D est le modèle *Toutin* (MT) développé au Centre canadien de télédétection, et le modèle empirique est basé sur les fonctions rationnelles (MRF) fournies par les vendeurs d'images. MFR post-traité avec un polynôme et MT ont été comparés pour les orientations des capteurs en utilisant un nombre variable de points d'appui (PA) dans la compensation par moindres carrés. MT et MFR avec Ikonos donnent des résultats équivalents à partir du moment où une translation, calculée avec au moins un PA, est appliquée au MFR. Par contre, MT donne de meilleurs résultats que MFR avec QuickBird, quelque soit le nombre de PA. Comme les MFR de QuickBird sont dépendantes du relief, des fonctions linéaires, calculées avec 6-10 PA, doivent lui être appliquées. De grandes erreurs en colonne ont, néanmoins, été décelées dans le MFR de l'image avant. Les altitudes des MNSs stéréo-extraites ont été ensuite comparées à des données Lidar (précision en altitude de 0,2 m). Comme la hauteur des couvertures du sol (arbres, maisons) est incluse dans l'altitude stéréo-extraite des MNS, les erreurs d'altitude avec un niveau de confiance de 68% ont été calculées pour la zone et pour trois couvertures de sol (forêts, urbaine/résidentielle, surfaces nues). MT et MFR avec Ikonos donnent des résultats semblables pour toutes les classes quelques soient la méthode et le nombre de PA. Par contre, MT donnent de meilleurs résultats que MFR avec QuickBird pour toutes les classes. Tous ces résultats démontrent le besoin de post-traiter les MFR d'Ikonos avec une translation tri-directionnelle et au moins un PA, mais celles de QuickBird doivent l'être avec une fonction linéaire et 6-10 PA.

1. INTRODUCTION

Due to high spatial resolution of these recent spaceborne sensors, a large number of researchers around the world have investigated (stereo-)photogrammetric methods using different physical and empirical models (Toutin, 2004a): 3D point positioning or feature extraction with empirical models (Di *et al.*, 2003; Tao *et al.,* 2004; Noguchi *et al.*, 2004; Fraser and Hanley, 2005) using manual/visual processes, and generation of digital surface models (DSMs) with physical models (Toutin, 2004b) or empirical models (Muller *et al.*, 2001; Lehner *et al.*, 2005) using automatic processes. The objectives of this paper are to expand on these results and compared 3D physical and empirical models for sensor orientations, point/elevation extraction and DSM generation. The physical model is the photogrammetric-based multisensor 3D geometric

* Corresponding author: thierry.toutin@ccrs.nrcan.gc.ca.

modeling (*Toutin's* model, TM) developed at the Canada Centre for Remote Sensing (CCRS) (Toutin, 1995) and adapted to HR stereo-images since 2000 (Toutin, 2004b). The empirical model is the rational function model (RFM) by applying the "so-called terrain-independent" approach using the RFM parameters provided by the image vendors (Madani, 1999). The paper evaluated the sensor-orientation and DSM quality when compared to accurate ground truth, and tracked the error propagation from the input data to the final DSMs. Different parameters affecting the process accuracy were also evaluated.

2. STUDY SITE AND DATA SET

2.1 Study Site

The study site is the Beauport, an area north of Québec City, Québec, Canada (47º N, 71º 30' W). This site is an urban, rural and forested environment and has a hilly topography with a mean slope of 7º and maximum slopes of 30º (Figure 1). The elevation ranges from 0 m at the St-Lawrence River to 450-m at a downhill ski mountains in the northern part (Figures 2 & 3).

Figure 1. Northern view of Beauport study site, Quebec with boreal forest and a hilly topography

Figure 2. Eastern night view of downhill ski station, Beauport study site with 350-m elevation range.

2.2 Data Set

Ikonos stereo images were distributed in a quasi epipolar-geometry reference where just the elevation parallax in the scanner direction remains (www.spaceimaging.com). For in-track stereoscopic image capture with the IKONOS orbit inclination, the image orientation approximately corresponds to a north-south direction, with few degrees in azimuth depending on the across-track component of the total collection angle. The ±27° in-track stereo images (10 km by 10 km; *B/H* of one) were acquired on 03 January 2001 when the sun illumination angle was as low as 19º, resulting in long shadows. The data were re-processed in April 2005 to obtain the RFM of Space Imaging (Grodecki, 2001). In addition, each image was subdivided in two sub-images generating two stereo-pairs (West and East) with a *B/H* of one, and had to be processed separately.

QuickBird stereo images, as a courtesy of Digital Globe, were provided as *Basic* imagery products, which are designed for users having advanced image-processing capabilities (http://www.digitalglobe.com). For users who did not develop or have access to a 3D physical geometric model, DigitalGlobe supplies QuickBird camera model information and RFM with each *Basic* Imagery product (Robertson, 2003). The ±29° in-track stereo images (18 km by 15 km; *B/H* of 1.1) were acquired 1 April 2003 when snow was still present in most of the bare surfaces, and a 45º-sun illumination angle results in shadows with vertical structures (Figure 3). The data were re-processed in July 2005 to take into account the new RFM improvement of DigitalGlobe (Cheng *et al.*, 2005). Figure 3 is the forward image, where general cartographic and topographic features are well identifiable: sand/gravel pits in A, snow-covered frozen lakes in B, snow-covered bare surfaces in C, power-line corridors in D and a mountain with downhill ski tracks in E.

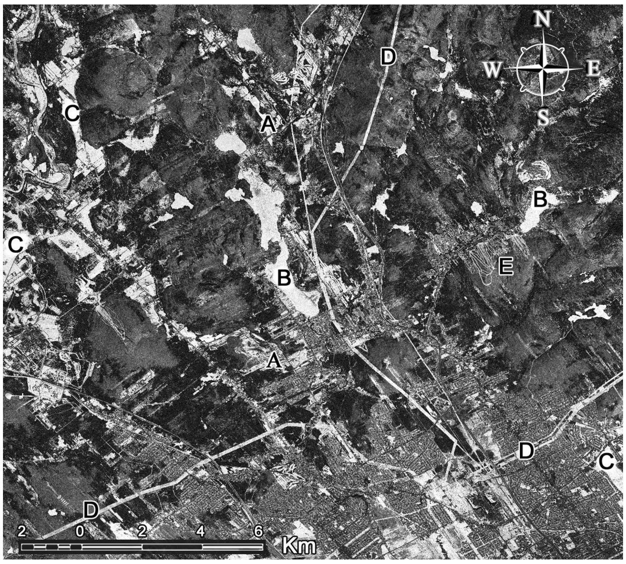

Figure 3. Forward QuickBird image (18 km by 15 km; 0.61-m pixel spacing), north of Québec City, Quebec, Canada acquired April 1, 2003. QuickBird Image © and Courtesy DigitalGlobe, 2003

To evaluate the accuracy of the stereo-extracted elevation of DSMs, accurate spot elevation data was obtained from a Lidar survey conducted by GPR Consultants (www.lasermap.com) on September 6^{th}, 2001. The Optech ALTM-1020 system is comprised of a high frequency optical laser coupled with a Global Positioning System and an Inertial Navigation System. The ground point density is about 300,000 3-D points per minute and the accuracy is 0.30 m in planimetry and 0.15 m in elevation (Fowler, 2001). Only ten swaths covering an area of 5 km by 13 km and representative of the full study site were acquired. The results of the Lidar survey are then an irregular-spacing grid (around 3 m), due also to no echo return in some conditions such as buildings with black roofs, roads and lakes. Since the objectives of this research study were to evaluate the stereo DSMs, the Lidar elevation data was not interpolated into a regular spacing grid so as to avoid the propagation of interpolation error into the checked elevation and evaluation.

3. EXPERIMENT

3.1 The 3D Physical and Empirical Models

The 3D physical model (CCRS-TM) was originally developed to suit the geometry of pushbroom scanners, such as SPOT-HRV, and was subsequently adapted as an integrated and unified geometric modeling to geometrically process multisensor images (Toutin, 1995), and HR images (Toutin, 2004b). This 3D physical model applied to different image types is robust and not sensitive to GCP distribution when there is no extrapolation in planimetry and elevation. Since TM is well explained in the previous references, only a summary is given. The geometric modeling represents the well-known collinearity condition (and coplanarity condition for stereo model), and integrates the different distortions relative to the global geometry of viewing. This 3D physical model has been applied to medium-resolution visible and infra-red (VIR) data (MODIS, Meris, Landsat 5 and 7, SPOT 1-5, IRS1-C/D, ASTER, Kompsat-1 EOC, ResourceSat-1), HR-VIR data (Ikonos, EROS, QuickBird, OrbView, SPOT5, Formosat-2, Cartosat), as well as radar data (ERS-1/2, JERS, SIR-C, Radarsat-1 and ENVISAT).

The 3D empirical model is the RFM, which is based on ratio of polynomial functions. The 3rd-order RFM, provided by the image resellers, were computed based on their own already-solved existing 3D physical models (calibration of internal orientation, sensor external orientation) (Grodecki, 2001). Since biases or errors still exist after applying the RFMs, the results need to be post-processed with few precise GCPs to compute 2D polynomial transformations (Fraser and Hanley, 2005), or the original RF parameters can be refined with linear equations requesting more precise GCPs (Lee *et al.* 2002).

3.2 The Processing Steps

Since the processing steps of DSM generation using either in-track or across-track stereo images are well known, the processing steps, including the accuracy evaluation are summarized in Figure 4:

1. Acquisition and pre-processing of the remote sensing data (images and metadata) to determine an approximate value for each parameter of 3D physical model for the two images;
2. Collection of stereo GCPs with their 3D cartographic coordinates and two-dimensional (2D) image coordinates. GCPs covered the total surface with points at the lowest and highest elevation to avoid extrapolations, both in planimetry and elevation. There were 34 and 48 collected ground points for Ikonos and QuickBird, respectively (2-3 m accuracy in the three axes). Due to the GCP definition in such area, the image pointing accuracy was around one pixel in cities and two pixels in mountainous areas.
3. Computation of the stereo models, initialized with the approximate parameter values and refined by an iterative least-squares bundle adjustment (coplanarity equations) with the GCPs (Step 2) and orbital constraints. Both equations of colinearity and coplanarity are used as observation equations and weighted as a function of input errors. Theoretically 3-6 accurate GCPs are enough to compute the stereo model, but more GCPs were acquired either to have an overestimation in the adjustment and to reduce the impact of errors or to perform accuracy tests with independent check points (ICPs).
4. Extraction of elevation parallaxes using multi-scale mean normalized cross-correlation method with computation of the maximum of the correlation coefficient;
5. Computation of *XYZ* cartographic coordinates from elevation parallaxes (Step 4) using the previously-computed stereo-model (Step 3) with 3D least-squares stereo-intersection;
6. Generation of regular grid spacing with 3D automatic and 3D visual editing tools: automatic for blunders removal and for filling the small mismatched areas and visual for filling the large mismatched areas and for the lakes; and
7. Statistical evaluation of the stereo-extracted elevations with the checked Lidar elevation data to compute the accuracy (linear error with 68% confidence level, LE68).

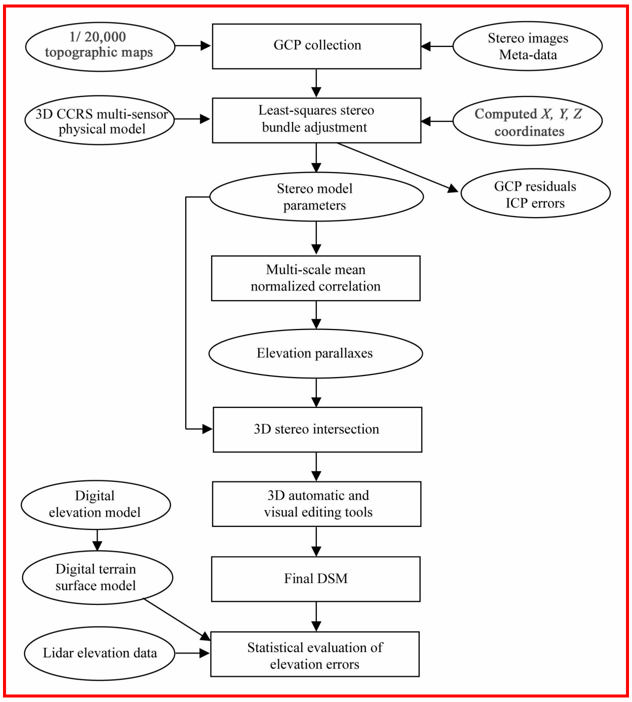

Figure 4. Processing steps for the generation of DSMs from stereo-images and their evaluation with Lidar data

In order to compare the impacts of CCRS-TM and RFM on the full stereo-processing, different tests applying each model using various numbers of GCPs were performed for each stereo-pair (Ikonos and QuickBird):

1) TM was computed with 10 and all GCPs (TM-10 and TM-all, respectively);
2) Supplied RFMs were directly applied (RFM); and
3) Supplied RFMs were refined using zero-order polynomial functions (shift) computed with one GCP (RFM-1);
4) Supplied RFMs were refined using first-order polynomial functions (linear) computed with 6, 10 and all GCPs (RFM-6; RFM-10; RFM-all, respectively).

The DEM is then evaluated with the Lidar elevation data. About 5 000 000 points corresponding to the overlap area were used in the statistical computation of the elevation accuracy.

Different parameters (land cover and its surface height), which have an impact on the elevation accuracy, were also evaluated.

4. RESULTS

4.1 Results on Sensor Orientations

Table 1 summarizes all results on sensor orientations of Ikonos/QuickBird using an iterative least-squares adjustment for the stereo-model computation. The different tests correspond by varying the number of GCPs: the results given in the image space (*x* column and *y* row in metres) are the GCP root-mean-square (RMS) residuals (for all tests) and the RMS errors at the remaining ICPs when available (e.g., TM-10, RFM, RFM-1, RFM-6, RFM-10).

StereoPair	Ikonos				QuickBird			
Test Nb. and Code	GCP		ICP		GCP		ICP	
	x	*y*	*x*	*y*	*x*	*y*	*x*	*y*
1) TM-10	0.5	0.4	1.8	1.8	0.7	0.7	1.5	1.4
1) TM-all	1.2	1.5	---	---	1.2	1.3	---	---
2) RFM	---	---	3.7	3.6	---	---	68	2.0
3) RFM -1	0.0	0.0	1.7	1.8	0.0	0.0	5.5	2.4
4) RFM-6	0.5	0.8	1.8	1.9	4.9	1.4	4.5	1.3
4) RFM-10	1.3	1.2	1.8	1.9	3.1	1.3	2.6	1.3
4) RFM-all	1.6	1.6	---	---	1.4	1.3	---	---

Table 1. Results on sensor orientations of Ikonos/QuickBird by an iterative least-squares adjustment for the stereo-model computation of both physical and empirical models. The number in the code tests correspond to the number of GCPs used. RMS residuals at GCPs and RMS errors at remaining ICPs are in the image space (*x* column and *y* row in metres)

Tests 1 confirmed previous results on the applicability of the physical model, TM, to stereo HR data. When there are more GCPs than the minimum required for computing a 3D physical model, the residuals mainly reflect the error of the input data, and, it is thus normal and "safe" to obtain residuals from the least-squares adjustment in the same order of magnitude as the GCP/ICP error (1-2 m), but the internal modeling accuracy is thus better, in the order of sub-pixel (Toutin, 1995, 2004b).

Tests 2 (RFM with no refinement) demonstrated and confirmed that the supplied RFMs (both for Ikonos and QuickBird) cannot achieve meter accuracy. The 68-m ICP error in column for QuickBird is due to the forward image (90 m) while the backward image has only 10 m error. Since TM and Test 2) RFM (ICP error in line direction of 2 m) gave good results with QuickBird, a tentative explanation in this large error is an error in the RFM generation in column direction. However, errors of 3-4 m for Ikonos and 2 m for QuickBird can be acceptable for some applications in remote areas where no control is available.

Because there was no improvement on ICPs when using 1^{st}–order polynomial functions computed with 6 or 10 GCPs for Ikonos (e.g., Tests RFM-6 and RFM-10), these two last tests (3 and 4) confirmed previous experiments on point positioning (Fraser and Hanley, 2005) that just a bi-directional shift (such as in Test RFM-1) is enough to improve supplied RFM of Ikonos to 1-2 pixels. On the other hand, the supplied RFM of QuickBird has to be refined at least with 1^{st}-order polynomial functions computed with 6-10 GCPs because the results of Tests 4 improved significantly when compared to results of Tests 2 (no refinement) and 3 (refinement with shift only). The largest errors in column for the different QuickBird tests were still due to the error in RFM generation of the forward image. The ICP error in line direction (1-2 m) indicated the potential of using RFM if there were no error in the RFM generation in column direction. These results confirm the previous experiments (Cheng et al., 2005) using linear functions for refining QuickBird RFM, but contradict other experiments (Nogochi et al., 2004; Fraser and Hanley, 2005) where a shift with or without a time-dependent drift, respectively was used. In fact, Fraser's results (2005), which mentioned time-dependent drift did not correct for systematic errors, were already in contradiction with results of his previous co-author (Nogochi et al., 2004), who demonstrated that a linear drift has to be added to the shift for correcting some "unexplained" systematic errors. Apart of the error in RFM generation a likely explanation for these contradictions on QuickBird RFM refinement is mainly the RFM dependency to terrain relief. As a matter of fact, Cheng's and our study site were 1000 m and 450 m elevation range, respectively (1st-order polynomial refinement), while Noguchi's study site was 240 m elevation range (shift and time-dependent drift refinement) and Fraser's study site 50 m elevation range (shift refinement).

4.2 Results on Elevation Extraction of DSMs

The second results are quantitative evaluations of DSMs (1-m pixel spacing) extracted from the two stereo pairs. The evaluations are related to the transversal parallaxes between the epipolar-images, the matching successes (Table 2) and to the comparison of DSMs with Lidar elevation data to compute the linear errors with 68% level of confidence (LE68) (Figures 5 and 6). LE68 were computed for the entire overlap areas and for the three classes (forested, urban/residential and bare surface).

Stereo Pair	Ikonos		QuickBird	
Test Nb. and Code	Trans. Parallax	Match Success	Trans. Parallax	Match Success
1) TM-10	< 1 line	89%	< 1 line	85%
1) TM-all	< 1 line	89%	< 1 line	85%
2) RFM	< 1 line	92%	150 lines	11%
3) RFM-1	< 1 line	92%	21 lines	31%
4) RFM-6	< 1 line	92%	16 lines	38%
4) RFM-10	< 1 line	92%	13 lines	50%

Table 2. Results on elevation extraction and DSM generation from Ikonos/QuickBird stereo-images: transversal parallaxes between the quais-epipolar images (in lines) and matching success on the image correlation (in percentage)

Table 2 showed that results (transversal parallaxes between epipolar images and matching success of the image correlation) are equivalent when using TM or RFM with Ikonos regardless of the number of GCPs. Because there is no transversal parallax between the epipolar images, resulting from a sub-pixel accurate stereo-modeling (Table 1), the matching has a very high success rate even with this challenging Ikonos stereo-pair. Same remarks applied to results when using TM with

QuickBird. Most of the mismatched areas correspond to snow-covered frozen lakes and shadowed areas due to a low solar illumination angle in January or April. On the other hand, RFM results are poor. The transversal parallaxes between the epipolar images, however, well reflected and are correlated with the RMS errors of the stereo-modeling (Table 1): the larger was the RMS errors, the larger is the transversal parallaxes. The consequence was of course a bad matching success with a one-direction correlation method or even with other methods.

In the elevation comparison with Lidar, some biases (3-7 m) were found but they can easily be corrected with at least an elevation control point. However, a large part of the biases (except for Test 2) RFM with QuickBird) were due to the trees height and it was confirmed when computing biases (around 1-2 m) for the bare surface areas. In fact, the supplied RFMs should thus be refined during the sensor orientation with a specific 3D polynomial functions (zero or first order) integrating a tri-directional shift (only the Z-parameter).

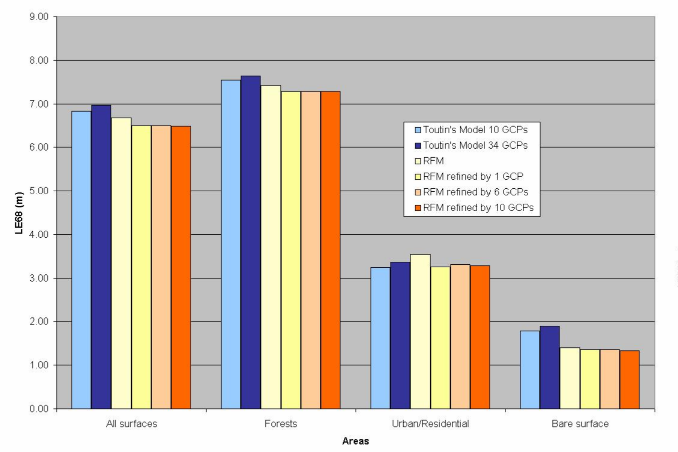

Figure 5. Statistical results computed from the difference between the Lidar elevation data and the stereo-extracted elevations of Ikonos DSM: the linear errors with 68% level of confidence (LE680 in metres) for the full overlap area (all classes), the forest, the urban/residential and the bare surface classes

Figure 5 showed the other statistical results of the comparison Lidar/Ikonos elevations: the different LE68 are relatively equivalent (few percent difference but not significant) indifferently when using TM or RFM regardless of the number of GCPs and the land cover class. Some general trends can be derived:

- Both TM and RFM performed well with stereo Ikonos;
- The number of GCPs do not affect the elevation accuracy for TM and RFM;
- RFM with 1st-order linear refinement does not improve elevation extraction and DSM accuracy;
- RFM without GCP being less accurate could still be an appropriate method for DSM generation in remote area without control;
- Refining RFM with a shift and GCP is the solution with few GCPs (1-3); and
- TM and RFM can be indifferently used when more GCPs are available.

Figure 6 showed the other statistical results of the comparison Lidar/QuickBird elevations: the different LE68 are much better when using TM than RFM for all GCP tests. Since LE68 over all surfaces for RFM was large (more than 210 m), it was not useful to compute the statistics for the other sub-classes. These differences between TM and refined-RFM LE68 are consistent for the three other land cover classes: on bare surface areas TM is almost twice better than RFM. Some general trends can also be derived:

- TM performed well with stereo QuickBird in regard to sensor resolution and stereo-geometry (*B/H* of 1.1);
- The potential error in RFM forward image is maybe the cause of the bad performance of the RFM with stereo QuickBird;
- The number of GCPs does not affect the elevation accuracy for TM but does for RFM;
- RFM refined with only a shift did not achieve good results (14 m on bare surface) in regard to sensor resolution and stereo-geometry (*B/H* of 1.1);
- For achieving the best results with RFM, a refinement with 1st-order linear functions and 6-10 GCPs is mandatory.

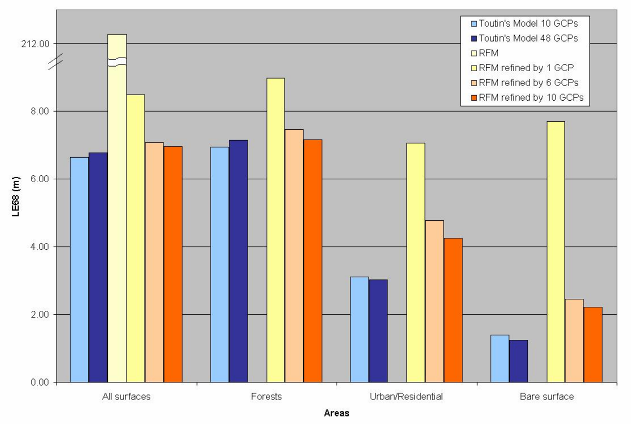

Figure 6. Statistical results computed from the difference between the Lidar elevation data and the stereo-extracted elevations QuickBird DSM: the linear errors with 68% level of confidence (LE68 in metres) for the full overlap area (all classes), the forest, the urban/residential and the bare surface classes

Finally, the results (Figures 5 and 6) over bare surface areas (1-2-m LE68), except when using RFM with QuickBird, better demonstrated the Ikonos/QuickBird stereo performance for 3D point/feature extraction and the potential to generate 5-m contour lines with the highest topographic standard. For the residential class, the results are a little worse because 1- and 2-storey houses (10 to 15 percent of the residential areas and 4 to 6 m in height) degrade the statistics a bit for this class.

5. CONCLUSIONS

The objectives of the research were to compare 3D physical and empirical geometric models for extracting elevation and generating DSMs from two in-track QuickBird and Ikonos stereo pairs (*B/H* of around 1) acquired over a residential/rural hilly area in Quebec, Canada. The first results on sensor orientations confirmed that TM and RFM with Ikonos gave equivalent results, as soon as supplied RFM is refined with a shift and one GCP. Larger polynomial order and number of GCPs did not improve the accuracy. On the other hand TM better performed than RFM with QuickBird regardless of the polynomial order and GCP number used in RFM refinement. Large unexplained error (68 m) was, however, noticed for the RFM (in column only) of the forward image. In conjunction with previous experiments, the results also confirmed that QuickBird RFM is thus relief dependent: the stronger is the relief the larger should be the polynomial order and the number of GCPs to refine the RFM.

The stereo-extracted elevation for generating DSMs were then compared to accurate elevation Lidar checked data. Because the surface heights were included in terrain elevation, the elevation errors were also evaluated and compared as a function of the land cover (forested; urban/residential; bare surface). The best results (TM/RFM Ikonos and TM QuickBird: 1-2-m LE68) were obtained on bare surfaces, where there was no elevation difference between the stereo-extracted and Lidar elevations. They are thus a good indication of HR stereo performance for 3D point/feature extraction and DSM generation. Because both TM and RFM performed well with stereo Ikonos and the number of GCPs did not affect LE68, the math model to be chosen is thus dependent on GCP availability. RFM with Ikonos is thus more useful when no control is available.

On the other hand, TM performed much better than RFM with stereo QuickBird. RFM, regardless of its refinement, achieved bad results in regard to sensor resolution and stereo-geometry (*B/H* of 1.1) but LE68 improved when RFM were refined with larger polynomial order and more GCPs. RFM with QuickBird could be useful when no control is available if there were no error in their generation. The results on elevation extraction and DSM confirmed then the results on sensor orientations related to the necessity to refine Ikonos RFM with a shift and one GCP only, and QuickBird RFM with 1st order linear functions and 6-10 GCPs.

The QuickBird RFM problems (potential errors in supplied RFM, post-processing, 6-10 GCP requirement, inconsistent results in different experiments and study sites, relief dependency) thus reduced the advantages of the "so-called terrain-independent" RFM approach versus a physical model in operational environments. Some explanations based on these and previous experiments for these results (sensor orientations and DSM) are inherent to the nature of physical and empirical models:

- RFMs are better suited for pre-processed map-oriented images with less geometrical/terrain distortions of small sizes, such as Ikonos *Geo* images; and
- Physical models, such as TM or other, are better suited for raw orbit-oriented images regardless of the size and the terrain and with the possibility of using metadata (ephemeris, attitude, etc.), such as QuickBird *Basic* images, which are still in the original viewing geometry.

ACKNOWLEDGEMENTS

The authors thank DigitalGlobe for providing the stereo QuickBird images, Mr. Réjean Matte of the *Ministère des Ressources naturelles du Québec*, Canada for the topographic data and GPR Consultants, Canada for the Lidar survey. They also thank M. Philip Cheng for integrating *Toutin's* model into OrthoEngine^{SE} software of PCI.

REFERENCES

Cheng, Ph, D. Smith, S. Sutton, 2005. Mapping of QuickBird Images: Improvement in Accuracy Since Release of First QuickBird, *GeoInformatics*, June, 8, pp. 50-52.

Di, K., R. Ma, R. Li, 2003. Geometric processing of Ikonos stereo imagery for coastal applications, *Photogrammetric Engineering & Remote Sensing*, 69(8), pp. 873-879.

Fowler, R.A., 2001. The Thorny Problem of Lidar Specifications, *Earth Observation Magazine*, 10(4), pp. 13-17.

Fraser, C. S., H.T. Hanley, 2005. Bias-compensated RPCs for Sensor Orientation of High-Resolution Satellite Imagery, *Photogrammetric Engineering & Remote Sensing*, 71(8), pp. 909-915.

Grodecki, J., 2001. IKONOS Stereo Feature Extraction – RPC Approach, ASPRS Annual Conference, St Louis, Missouri, USA, April 23-27 (Bethesda, MD: ASPRS), CD-ROM.

Lee, J.-B., Y. Huh, B. Seo, Y. Kim, 2002. Improvement the Positional Accuracy of the 3D Terrain Data Extracted From IKONOS-2 Satellite Imagery, *International Archives of Photogrammetry and Remote Sensing*, Graz, Austria, September 9-13 Vol. 34 (B3), pp. B142- B145.

Lehner, M., R. Müller, P. Reinartz, P., 2005. DSM and Orthoimages from QuickBird and IKONOS Data using Rational Polynomial Functions, *The International Archives of Photogrammetry and Remote Sensing*, Hannover, Germany, May 17-20. Vol. 36 (Part1/W3), CD-ROM.

Madani, M., 1999. Real-Time Sensor-Independent Positioning by Rational Functions, *ISPRS Workshop on Direct Versus Indirect Methods of Sensor Orientation*, Barcelona, Spain, November 25-26 pp. 64-75.

Muller, J.-P., J.-R. Kim, L. Tong, 2001. Automated mapping of surface roughness and landuse from simulated and spaceborne 1m data, *Automatic Extraction of Man-Made Objects From Aerial and Space Images (III)*, A.A. Balkema, Rotterdam, The Netherlands, pp. 369-379.

Noguchi, M., C. S. Fraser, T. Nakamura, T. Shimono, S. Oki, 2004. Accuracy Assessment of QuickBird Stereo Imagery, *Photogrammetric Record*, 19(106), pp. 128-137.

Robertson, B., 2003. Rigorous Geometric Modeling and Correction of QuickBird Imagery, *IGARSS 2003*, Toulouse, France, 21-25 July 2003, CD-ROM.

Tao, C.V., Y. Hu, W. Jiang, 2004. Photogrammetric exploitation of IKONOS imagery for mapping application, *International Journal of Remote Sensing*, 25(14), pp.2833-2853.

Toutin, Th., 1995. Generating DEM from Stereo-Images with a Photogrammetric Approach: Examples with VIR and SAR data, *EARSeL Advances in Remote Sensing*, 4(2), pp. 110-117.

Toutin Th., 2004a. Review Paper: Geometric processing of remote sensing images: models, algorithms and methods, *International Journal of Remote Sensing*, 25(10), pp. 1893-1924.

Toutin, Th., 2004b. Comparison of Stereo-Extracted DTM from Different High-Resolution Sensors: SPOT-5, EROS, IKONOS and QuickBird, *IEEE-TGARS*, 42(10), pp. 2121-2129.